International Journal of Mechanical Engineering (IJME)
ISSN (P): 2319-2240; ISSN (E): 2319-2259
Vol. 7, Issue 3, Apr-May 2018; 31-40

International Academy of Science, Engineering and Technology
Connecting Researchers; Nurturing Innovations

COMPARISON BETWEEN 4 BLADE, 6 BLADE AND 20 BLADE IMPELLER BY USING CFD ANALYSIS OF A RESPIRATOR

Suresh. P & Mohammed Mussa

Department of Mechanical Engineering, Jig-Jiga University, Jig-Jiga, Ethiopia

ABSTRACT

An impeller design for a respirator is addressed in several textbooks and research articles. According to practiced methods, the overall dimensions and properties of an impeller can be determined using computational fluid dynamics (CFD) and thermodynamic relations. Designing impeller for a respirator is important for fluid flow analysis. The impeller meridional profile is an important detail as a significant influence on the performance. Four, Six blade impellers are commonly used in the industries presently. In this study; I have proposed 20 blade impeller, in order to increase the outlet flow velocity and cutting down the cost. Also, Comparison between these impellers is made in respect of other aspects like material, outlet velocity, fluid discharge, and efficiency. The material used for 4, 6 blade impellers is steel and the material used for 20 blade impeller is Acrylonitrile butadiene styrene (ABS) which is used to reduce noise and cutting down the cost of the impeller.

***KEYWORDS**: Computational Fluid Dynamics (CFD); 4 Blade Impeller; 6 Blade Impeller, 20 Blade Impeller, Respirator*

Article History

***Received:** 7 Mar 2018 | **Revised:** 2 Apr 2018 | **Accepted:** 7 Apr 2018*

1. INTRODUCTION

Respirators are widely used in the industries, painting works, mines, toys and where the air required with a certain velocity by using an impeller. An impeller (also written as impellor or impellar) is a rotor used to increase the pressure and flow of a fluid. Impellers (also spelled impellors or impellars) are rotating devices designed to alter the flow and/or pressure of liquids, gases, and vapors. Impellers consist of various vanes — often blade-shaped — arranged around a short central shaft. When the shaft and vanes rotate, they suck in fluids or gases and impel them out the other side. The image below illustrates basic impeller operation. Impellers simply consist of a series of vanes attached to a central "hub" designed to be fitted to a shaft. By fitting the vane ends very close to the casing, the impeller is able to prevent large amounts of fluid or gas from recirculating back through the eye. A wide variety of impeller types have been constructed and used in many different applications in industry and other technical sectors. However, their design and performance prediction process is still a difficult task, mainly due to the great number of free geometric parameters, the effect of these cannot be directly evaluated. The significant cost and time of the trial-and-error process by constructing and testing physical prototypes reduces the profit margins of the respirator manufacturers. For this reason, CFD analysis is currently being used in the design and construction stage of various impellers types. The experimental way of impeller test can give the actual value of head developed, power rating and efficiency. But the internal flow conditions cannot be predicted by the

experimental results. From the CFD analysis software and advanced post-processing tools the complex flow inside the impeller can be analyzed. The complex flow characteristics like inlet pre-swirl, flow separation and outlet recirculation cannot be visualized by the experimental way of pump test. But in the case of CFD analysis, the above flow characters can be visualized clearly.

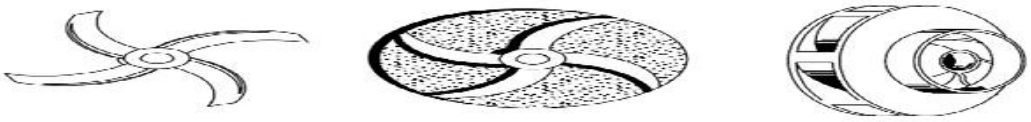

Figure 1: 4 Blade Impeller

Computational fluid dynamics (CFD) analysis is being increasingly applied in the design of impellers for a respirator. With the aid of the CFD approach, the complex internal flows in air pumping impellers, which are not fully understood yet, can be well predicted, to speed up the impeller design procedure. Thus, CFD is an important tool for impeller designers. The use of CFD tools in turbo machinery industry is quite common today. Many tasks can numerically be solved much faster and cheaper than by means of experiments. Nevertheless, the highly unsteady flow in turbo machinery raises the question of the most appropriate method for modeling the rotation of the impeller.CFD analysis is very useful for predicting pump performance at various mass-flow rates. For designers, prediction of operating characteristics curve is most important. All theoretical methods for prediction of Efficiency merely give a value; but one is unable to determine the root cause of the poor performance.

The purpose of the 4, 6 blade impeller is to show a numerical study of a respirator impeller taking into account the whole 3-D geometry and the unsteadiness of the flow. It has been done with the commercial software package CFD. The code uses the finite volume method and solves the k-ε equations with the ability to handle unstructured grids, include relative reference frames and make unsteady calculations with moving meshes [1].

Figure 2: 6 Blade Impeller

Impellers are prevalent for much different application in the industrial or other sectors. Nevertheless, their design and performance prediction process is still a difficult task mainly due to the great number of free geometric parameters, the effect of which cannot be directly evaluated. The significant cost and time of the trial and error process by manufacturing and testing of physical prototype reduces the profit margins of the impeller manufacturers. For this reason, CFD analysis is currently used in hydrodynamic design for different impeller types. An impeller is a rotating part of a respirator that imparts kinetic energy to a fluid. Here under we introduced (1) modeling laws and (2) Vibration and noise [2].

The Modeling Laws include both the affinity law and model law. These two laws are stated as Affinity Law "for similar conditions of the flow the capacity will vary directly with the ratio of speed and/or impeller diameter and the head with the square of this ratio at the point of best efficiency".

Model Law **"**two geometrically similar pumps working against the same head will have similar flow conditions if they run at speeds inversely proportional to their size, and in that case, their capacity will vary with the square of their size".

According to Bernoulli, the differential pressure equation is given by

$$\frac{P_1}{\circ} + \frac{V_1^{\,2}}{2} + Z_1 g = \frac{P_2}{\circ} + \frac{V_2}{2} + Z_2 g \tag{1}$$

$V_2 = 0$; $Z_1 = Z_2$.

The difference pressure equation is given by

$$(P_2 - P_1) = \frac{V^{\,2} * \circ}{2} \tag{2}$$

Where

P_1 =Initial pressure at the inlet of the impeller, in bar

P_2 = Final pressure at the outlet of the impeller, in bar

ρ = Density of air in kg/m^3

V =Velocity of air in m/s

2. GOVERNING EQUATIONS

CFD applies numerical methods called discretization to develop approximations of the governing equations of fluid mechanics and the fluid region to be studied. The set of approximating equations is solved numerically for the flow field variables at each node [3].

$$\frac{\partial}{\partial t}\int_v \rho\, \emptyset dv + \oint_A \rho \emptyset V . dA = \oint_A \Gamma \nabla \emptyset . dA + \int_V s_\emptyset \, dV$$

<Unsteady> + <Convention> = <Diffusion> + <Generation>

To keep the details simple, we illustrate the fundamental ideas underlying CFD by applying them to the following simple first order differential equation:

$$\frac{du}{dx} + u_m = 0; 0 \le x \le 1; u(0) = 1 \tag{3}$$

It first considers the case where *m* = 1 when the equation is linear. This later considers the case where m= 2 when the equation is nonlinear. This derives a discrete representation of the above equation with *m* = 1 on the following grid:

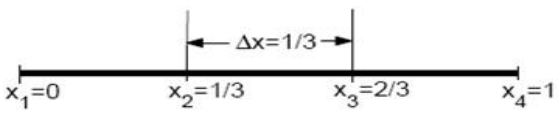

This grid has four equally-spaced grid points with Δx being the spacing between successive points. Since the governing equation is valid at any grid point, we have

$$\left[\frac{du}{dx}\right]_i + u_i = 0. \quad (4)$$

Here the subscript *i* represents the value at the grid point x_i . In order to get an expression for (*du/dx) i* in terms of *u* at the grid points, we expand u_{i-1} in Taylor's series as

$$u_{i-1} = u_i - \Delta x \left[\frac{du}{dx}\right] + o(\Delta x^2). \quad (5)$$

A simple rearrangement of (5) gives

$$\left[\frac{du}{dx}\right]_i = \frac{u_i - u_{i-1}}{\Delta x} + o(\Delta x). \quad (6)$$

The error in $(du/dx)_i$, due to the neglected terms in Taylor's series, is called the truncation error. Since the truncation error is $O(\Delta x)$, this discrete representation is termed first order accurate. Using (6) in (5) and excluding higher-order terms in Taylor's series, we get the discrete equation as [4]

$$\frac{u_i - u_{i-1}}{\Delta x} + u_i = 0 \quad (7)$$

This method of deriving the discrete equation using Taylor's series expansions is called the finite-difference method. However, most commercial CFD codes use the finite-volume or finite-element methods which are better suited for modeling flow past complex [5].

3. CFD PROCEDURE AND ANALYSIS

Fluid flow analysis performed on the impeller, using ANSYS CFX. Numerical results fully characterized the flow field, providing detailed flow information such as flow speed, flow angle, pressure, boundary layer development, losses [6]. The flow field information from CFD simulation was then used to help elucidate the flow physics. Impeller, blade geometry is shown in figure 2. Design specification of 6 blades and 20 blades impellers are shown in table 1 and table 2.

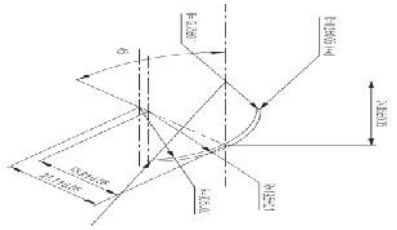

Figure 3: Blade Geometry of Impeller

Table 1: Design Specification of 4, 6 Blade Impeller and 20 Blade Impeller

S.No	Parameter	4 Blade Impeller	6 Blade Impeller	20 Blade Impeller
1	Inlet diameter (D_i)	65 mm	52 mm	22.67 mm
2	Outlet diameter(D_0)	130 mm	104 mm	67.74 mm
3	Blade number	4	6	20
4	Inlet angle (α)	75^0	73.5^0	38^o
5	Outlet angle (β)	58^0	56.5^0	62^0
6	Blade thickness (t)	4 mm	3mm	2.5 mm
7	Shaft diameter (D_s)	12 mm	14 mm	6 mm

3.1 Meshing of Impeller Blades

Turbo grid uses unstructured meshes in order to reduce the amount of time spent generating meshes. The geometry modeling and mesh generation processes simplifying model more complex geometries that can be handled with conventional Multi-block structured meshes. The mesh is adapted to resolve the flow-field features [7]. This flexibility allows picking mesh topologies that are best suited for the particular application. The geometry is created by using Solid Works and the extruded geometry is meshed by Turbo Grid. Meshing 20 blades Impeller is shown in Figure 3. Mesh statistics and comparison between 6 blades and 20 blades is shown in Table 2, Table 3 and Table 4.

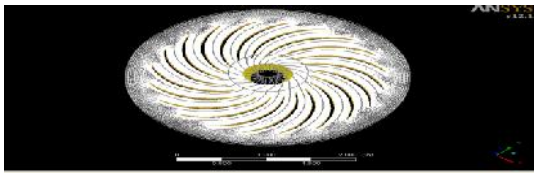

Figure 4: Meshing of 20 Blade Impeller

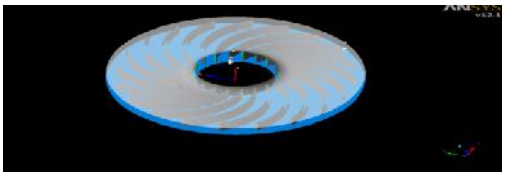

Figure 5: 20 Blades Impeller

Table 2: Mesh Statistics of 20 Blade Impeller

S. No.	Mesh Measure	Value
1.	Minimum face angle	27.3654
2.	Maximum face angle	173.265
3.	Maximum element	372,072
4.	Minimum volume	1,74683e-012 [inches]
5.	Maximum edge	1970.8

Table 3: Mesh Statistics 6 Blade Impeller

No. of Nodes	211637
No. of Elements	239456

Table 4: Comparison between 4, 6 Blade and 20 Blade Impeller

S. No.	Parameter	4 Blade Impeller	6 Blade Impeller	20 Blade Impeller	Benefits of New Model
1	Inlet angle	75^0	73.5^0	38^0	Flow increment
2	Outlet angle	58^0	56.5^0	62^0	Flow increment
3	Number of blades	4	6	20	Flow increment
4	Material	Steel	Steel	ABS (C_8H_8)	Cost reduction
5	Outlet velocity	19.32 m/s	23.22 m/s	32.46 m/s	Outlet velocity increment
6	Discharge	3.8 Lps	4.00 Lps	5.2 Lps	Discharge increased
7	Head	10 m	12 m	18 m	Head Increased

3.2 CFX Preprocessor

Impeller domain is considered as a rotating frame of reference with the different rotational speed of 10000RPM, 8000RPM, 6000 rpm, 4000 rpm, and 2000 rpm. The working fluid through the pump is water at 300k. K-ε turbulence model. Inlet static pressure and outlet mass flow rate 29.63 kg/mol. Three-dimensional incompressible N-S equations are solved with ANSYS-CFX Solver (for 20 blade impeller) [8].

Impeller domain is considered as a rotating frame of reference with the different rotational speed of 2842RPM, 2848RPM, 2858 rpm, 2866 rpm, and 2918 rpm [9]. The working fluid through the pump is water at 300k. K-ε turbulence model. Inlet static pressure and outlet different mass flow rate of 8.78 kg/s,6.83 kg/s, 6.25 kg/s,5.30 kg/s,0.00 kg/s are given as boundary conditions [10].

Three-dimensional incompressible N-S equations are solved with ANSYS-CFX Solver (for 4,6 blade impeller).

3.2.1 Wall Boundary Conditions

No-slip conditions were prescribed on the impeller blade surface. The Zero Neumann boundary condition was imposed for pressure at the walls.

4. RESULTS AND DISCUSSIONS

4.1 Span wise Velocity Contours at 10000 rpm at 20 %, 50% and 70% for 20 Blade Impeller

As Sean from figures 6 to 7, the velocity distribution varies as the speed of the impeller changes. Figure 8 represents high velocity (32.46 m/s). The flow separation takes place at the middle of the blade from inlet compare to 10000 rpm the flow separation takes place at the end of the blade. From the above figures tells if the speed of the impeller increases automatically velocity also increases.

Figure 6: Velocity Contour 20% at 10000 rpm

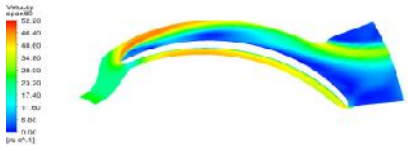

Figure 7: Velocity Contour 50% at 10000 rpm

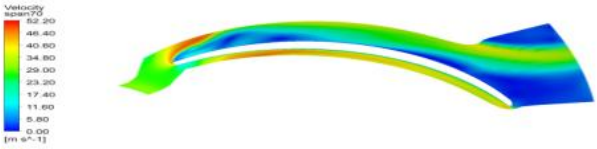

Figure 8: Velocity Contour 70% at 10000 rpm

4.2 Static Pressure Contours at 10000 rpm, at 20 %, 50% and 70% for 20 Blade Impeller

As Sean in the figures, the pressure distribution will varies as the speed of the impeller changes. From figure 11 the pressure at the inlet is as compared to the pressure at an outlet in 10000rpm case but in the 2000 rpm case the pressure at the inlet is low and the pressure at an outlet is high that means the exit velocity in 2000 rpm is low as compared to 10000rpm.

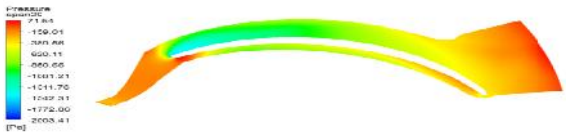

Figure 9: Static Pressure Contour 20% at 10000 rpm

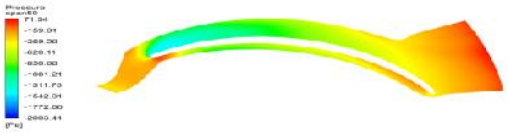

Figure 10: Static Pressure Contour 50% at 10000 rpm

Figure 11: Static Pressure Contour 70% at 10000 rpm

4.3 Total Pressure Contours at 10000 rpm at 20%, 50 % and 70% for 20 Blade Impeller

Figure 12: Total Pressure Contour 20% at 10000 rpm

Figure 13: Total Pressure 50% at 10000 rpm

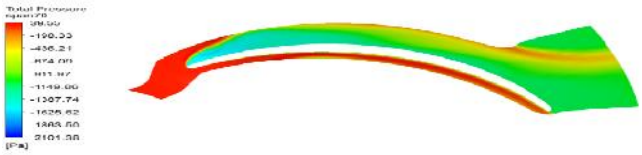

Figure 14: Total Pressure Contour 70% at 10000 rpm

4.4 Span wise Velocity Profiles at 10000 rpm, 8000 rpm, 6000 rpm, 4000 rpm and 2000

Profiles of span wise velocity component are shown in Figures for 10000 rpm, 8000 rpm, 6000 rpm, 4000 rpm and 2000 rpm respectively. The figures X- axis represents axial chord and Y- axis represents velocity in m/s. The figure represents flow variations in 10000rpm, 20%, 50%, 70% span wise.

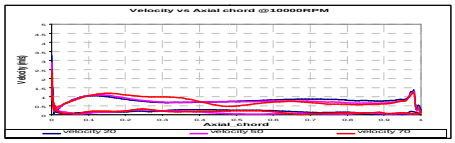

Figure 15

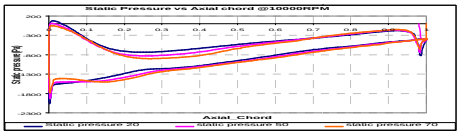

Figure 16

Figures 14 & 15: Velocity and Static Pressure Contours at 20%, 50% and 70% at 10000 rpm

Mean contours of span wise pressure components are shown in Figure 16 for 10000 rpm. The figure X- axis represents axial chord and the Y- axis represents pressure in Pa. The figure 16 represents flow variations in 10000 rpm at contours 20%, 50%, 70% span wise.

4.5 Mean Span wise Total Pressure Profiles for 20 Blade Impeller

Mean contours of span wise total pressure component are shown in Figures for 10000 rpm , 8000 rpm, 6000 rpm, 4000 rpm and 2000 rpm respectively. The figures X- axis represents axial chord and Y-axis represents total pressure in Pa. The figures represents flow variations in 10000 rpm , 8000 rpm , 6000 rpm , 4000 rpm and 2000 rpm at contours 20% , 50%, 70% span wise at an outlet.

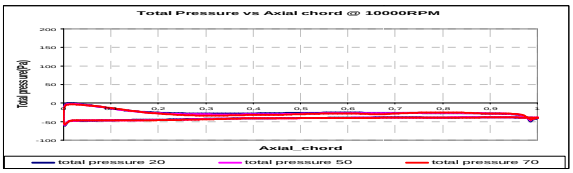

Figure 17

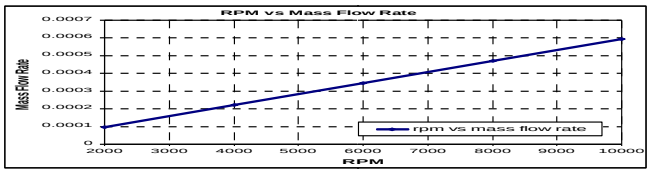

Figure 18

Figures 17 & 18: Total Pressure at 20%, 50% and 70% at 10000 rpm& Rpm vs Mass Flow Rate

From figure 18 shows at different rpms (10000, 8000, 6000, 4000 and 2000) the behavior of fluid flow at the outlet. If the rpm increases the flow at an outlet will also increase.

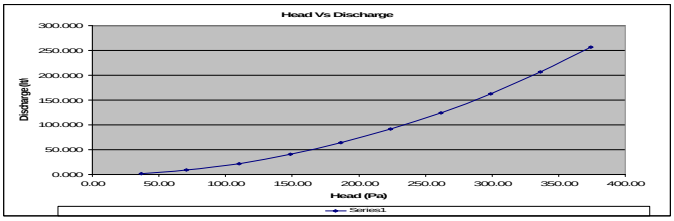

Figure 19: Head vs Discharge for 20 Blade Impeller

The graph shows head vs discharge-axis represents head in Pa and Y-axis represents discharge in m^3 /s. the above graph shows there is no formation of surge and stall.

5. CONCLUSIONS AND SCOPE

The proposed improvements include (a) Impeller & blade material to be changed (b) Number of blade increases (c) Blade inlet angle to be changed (d) Blade outlet angle to be changed (e) CFD software results compare with the classical and new model.

Compared to 4, 6 blade and 20 blade impeller, 20 blade impeller gives more discharge at the outlet of the impeller and also velocity obtained from the CFD predictions is 35.46 m/s. It has been observed that compared to these impellers 20 blade impeller is free from surge and stall. There is no formation of wake in 20 blade impeller. It has been observed that the velocity of the fluid is directly proportional to impeller's RPM. Correlation has been derived from Head and Discharge. Correlation has been derived from RPM and Mass flow rate.

Future work should involve advancing the solution further in time for dynamic inflow or outflow boundary condition; and all the present simulations may be performed on a finer grid. Grid refinement may be done in order to obtain accurate results in both span wise as well as pitch wise directions.

6. REFERENCES

1. *Baun D.O., Flack R.D. 2003. Effects of volute design and number of impeller blades on Lateral impeller forces and hydraulic performance, International Journal of Rotating Machinery, Vol. 2, No. 9, pp. 145-152.*
2. *Labanoff Robert R. Ross, Centrifugal blower impeller design & application Gulf Publishing Company, Houston, TX, 1992, volume-2.*
3. *T.E.Stirling: "Analysis of the design of two pumps using NEL methods" Centrifugal Pumps-Hydraulic Design-I Mech E Conference Publications 1982-11, C/183/82.*
4. *Numerical Calculation of the flow in a centrifugal blower impeller using Cartesian grid procedure of 2nd WSEAS int. Conference on applied and theoretical mechanics, Venice, Italy, November20-22,2006,According to john S.Anagnostopoulos.*
5. *PITTALA, SURESH, and T. DIRIBA. "COMPUTATIONAL FLUID DYNAMICS ANALYSIS OF IMPELLR DESIGN FOR A PUMP."*
6. *Young-Kyun Kim, Tae-Gu Lee, Jin-Huek Hur, Sung-Jae Moon, and Jae-Heon Lee World Academy of Science, Engineering and Technology 50 2009.*

7. *International Journal of Rotating Machinery 2005:1, 45–522005 Hindawi Publishing Corporation Mechanical and Fluids Engineering Department, Southwest Research Institute, 6220 Culebra Road, an Antonio, TX 78238-5166, USA.*
8. *MA Xi-jin, ZHANG Huachuan, ZHANG Kewei. Numerical Simulation and Experiment Analysis of Thirdly Circulating Feed-water Mixed-flow Pump in Nuclear Power Station. FLUID MACHINERY. Vol.37, No.09, 2009 6-9.*
9. *Georgiana DUNCA1, Sebastian MUNTEAN 2, Eugen Constantin ISBĂŞOIU3, U.P.B. Sci. Bull., Series D, Vol. 72, Iss. 1, 2010.*
10. *Miner S.M. 2001, 3-D viscous flow analysis of a mixed flow pump impeller, International Journal of Rotating Machinery, Vol. 7, No. l, pp. 53-63.*
11. *Prepared for the33rd Joint Propulsion Conference and Exhibit cosponsored by AIAA, ASME, SAE, and ASEE Seattle, Washington, July 6–9, 1997.*